Journal of Energy Challenges and Mechanics
http://www.nscj.co.uk/JECM/
ISSN 2056-9386
Volume 2 (2015) issue 4, article 4

Combined break-junction tunneling and STM/STS studies of the β-tungsten-type superconductor Nb_3Sn below and above T_c

对临界温度上下β-钨型超导体 Nb_3Sn 的破结穿隧与STM/STS之结合研究

Toshikazu Ekino[1*], Alexander M. Gabovich[2], Yuta Sakai[1], Akira Sugimoto[1]and Jun Akimitsu[3]

[1]*Hiroshima University, Graduate school of Integrated Arts and Sciences, Higashihiroshima739-8521, Japan*
[2]*Institute of Physics, National Academy of Sciences, Kiev 03680, Ukraine*
[3]*Aoyama-Gakuin University, Department of Physics, Sagamihara 252-5277, Japan*

ekino@hiroshima-u.ac.jp

Accepted for publication on 25 December 2015

Abstract **- Electron-tunneling spectroscopy was employed to investigate the well-knownβ-tungsten-type Nb_3Sn superconductor. The primary measurements were done by means of the surface-sensitive break-junction technique. BCS-like energy-gap features are reproduced in the superconducting state. Reproduced conductance humps outside the superconducting gap structures are commonly observed. Such hump structures are complementary to coherent peaks at the superconducting-gap edges and resemble the pseudo gap phenomena revealed in copper-oxide high-T_c superconductors. Those humps become the only gap-like manifestations above T_c. The possible origin is discussed in terms of the charge-density wave (CDW) formation associated with the structural phase transition. The scanning tunneling microscopy/spectroscopy (STM/STS) measurements were also carried out to obtain complementary density-of-states data.**

Keywords – **Tunneling, break junction, STM/STS, energy gap, A-15 compound, high-T_c superconductor.**

I. INTRODUCTION

One of the intriguing features of high-T_c superconductors is the manifestation of the gap-like structures above the superconducting critical temperature. This puzzling issue has been intensively investigated in terms of either the precursor Cooper-pairing effects or the competing phenomena suppressing the superconducting critical temperature [1]. The nature of the normal-state gap formation in cuprate high-$T_c$superconductors is not perfectly understood to date, althoughseveral possible origins were suggested based on the formation of competing charge density waves (CDWs) with accompanying periodic lattice distortions in the layered crystal structures. The CDW appearance in cuprate superconductorswas confirmed experimentally and theoretical attempts have been made to identify CDW manifestations with the observed tunnel and photoemission spectral data[1].It is natural to search for the existence of such phenomena in the other classes of superconductors with CDW anomalies occurring at temperatures both higher and lower than T_c.A-15 (β-tungsten) compound Nb_3Sn, which hadone of the highest superconducting critical temperatures, T_c, over a long periodbefore the discovery of high-$T_c$cuprate superconductors 30 years ago[2], is very promising in this connection.

This materialdoes not exhibit a layered crystal structure appropriate to cuprates.However,its lattice includes orthogonal linear chains of Nb atoms alongprincipal cube axis directions[2]. Such quasi-one-dimensional feature tends to induce structural anomalies driven by peculiarities of the normal-state electron density of states, $N(E)$, near the Fermi level, which determines T_c. Actually, A-15 materials undergo tetragonal distortions below certain temperatures,$T_m>T_c$.Hence, Fermi surface is partially gapped by concomitant CDWs, which is detrimental to superconductivity. Such an interplay between superconducting pairing and CDWswas intensively studied

for a number of A15 compounds both experimentally and theoretically, and Nb_3Sn ($T_c \approx 18$ K) isthe representativecase [3-5].The superconducting and CDW order parameters inevitably lead to the corresponding superposed energy gaps induced by both Cooper and electron-hole pairings. The origin of superconductivity and the gapping features of A-15 compounds wereeffectively explored by the conductance spectroscopy in the tunnel [6] and point-contact [7] regimes as the typical methods to probe these phenomena. The experiments revealed a single clear-cut superconducting gap, and another feature at higher voltages most probably connected to the structural transition [8].

In this paper, tunneling measurements of Nb_3Sn single crystals are presented using break-junction (BJ) [9] and the scanning tunneling microscopy/spectroscopy (STM/STS)techniques on the basis of the previous works [6, 8]. The experiments were carried out focusing on both the superconducting gap features and the electronic peculiarities of $N(E)$ emerging due to the structural (martensitic) transition intimately associated with CDWs. The mean-field equations describing competing superconducting and electron-hole pairings are the same for the majority of microscopic descriptions of the CDW pairings[1, 4, 5]. Therefore, the important consequencesare similar. One expectsthe manifestations of CDWs in the quasiparticle conductance $G(V) = dI/dV$, where I denotes the quasiparticle tunnel current across thejunction. The $G(V)$ curve in CDW superconductors is a complicated functional of the superconducting, Δ, and dielectric (CDW), Σ, energy gaps [1, 5, 10]. In the BJTS method,$G(V)$ doesnotinclude a simple convolution of the gapped electron density of states as in the conventional Bardeen-Cooper-Schrieffer (BCS) model of superconductivity.

II. Experimental procedures

Single crystalsof Nb_3Sn weregrown by a vapor transport method. The sample resistivitywasmeasuredin a standard dcfour-probeconfiguration. The main measurement techniques employed here were the tunneling spectroscopy using the break junction (BJTS) and the low-temperature ultra-high-vacuum(~ 10^{-8} Pa) STM/STS with a PtIr tip. In theBJTS technique, clean and unaffected superconductor – insulator – superconductor (SIS) junction interface can be obtained *in situ* along the crack of the tiny single-crystal piece at T = 4 K in the helium atmosphere. Thebreak junction configuration therefore possesses the gap peak-to-peak interval to be $4\Delta/e$ instead of $2\Delta/e$ of the superconductor – insulator – normal metal(SIN) junction, where e denotes the elementary charge. This relationships are also validwhen the gap has a dielectric (CDW) origin.The BJ tunneling spectra were measured using a low-frequency ac-modulation technique with a low-noise lock-in amplifier. When the junction wasmechanically stable, a long-period full bias-voltage scantaking 30 min – 1hr or more was adopted to eliminate any parasitic effects in the tunnel currents.

The main aim of adopting BJTS is to exploreverydelicate electronic properties using a conventionalsensitive technique, but we also carried out the STM/STS measurements in order to obtain further evidence detectingthe existence of the interplay between superconducting and CDW pairings.Here, the preliminary STM/STSresults are presentedtogether with the BJTS data.

III. Results and discussion

The temperature dependence of the resistivity forthe Nb_3Sn sample showed a sharpdrop at the superconductingtransition and becomes zero at T = 18.1 K, therebyindicating the sufficientquality of the test sample.

Whatever the details, knowing high T_c of Nb_3Sn, we should analyze its gapstructuresbearing in mindthe expected strong-coupling nature of the superconducting electron pairing. Here the BJTS resultsareshown inFigure 1 for severaldifferentjunctions.The data shown here constitutearepresentative group among junctions with similar characteristics. One can see the main gap peaks at ± 2.0 – 2.2 mV and broad peaks at ± 2.8 – 3.0 mV. Assuming the SIS nature of the junction, these values correspondto ± $2\Delta/e$.Sometimes the double-peaked gap structures including both peak values (± 2.0 and ± 2.8 mV) are observed. This two-gap feature qualitatively resembles the two-band superconductivity as reported also in $Nb_3Sn$by point-contact spectroscopy measurements[11]. In our case, the second gap valuesscatter substantially although the basic-gap value is almost the same.Thus, we did observe the double-gap structures but in most cases the single-gap feature was found showing either≈ 3 mV or ≈ 2 mV values.The latter characteristics always demonstrate sharp gap structures as is shown in the figure. Therefore, we could not identify, which of the observed gaps is intrinsic for this compound.

The $G(V)$ curve with the smaller gap and distinct conductance structurecorresponds to the standard BCS quasiparticle density of states $N(E,\Gamma) = |\mathrm{Re}\{(E-i\Gamma)/[\Delta^2-(E-i\Gamma)^2]^{1/2}\}|$, where E is the energy, Γ is aphenomenological broadening parameter [12].The value of energy gap, 2Δ, was found by fitting the SIS conductance, determined by the convolution of two $N(E,\Gamma)$ factors. It gives the gap-peak energy, regardless of the Γ value [13] .In the fitting, we included the thermal smearing effect in addition to Γ broadening. Similar gap-peak positions were foundalthough the spectra are of different quality. The gap values thus obtained are $2\Delta(4K)$ = 2 – 2.8meV. The results therefore reveal the gap ratio $2\Delta/k_BT_c$ = 2.8 – 3.6, which is in the range of the *s*-wave-pairing BCS ratio 3.52. The value, which is smaller than the BCS one, indicatesthe existence of the local non-stoichiometriclow-T_c region.The secondary gap features were also observed in the novel iron-based binary superconductors, and discussed in connection with either the local off-stoichiometric effect or the multi-gap superconductivity [14].

In the middle experimental curve of Fig. 1, the intensive dipstructures are observed at ± 12 mV. Such features were often attributed to the manifestation of the strong electron-phonon interactionexpected for this compound

[15].However, it should not be the case here, becauseof irreproducibility andan unusual depth of the dips as comparedwith the strong-coupling features. Instead, thedipsare probably generated by the proximity effects and/or the weak-link behavior in the local patches of thejunction area.

For higher bias voltages at the same fixed T = 4. 2K, one can observe shoulders or hump structures at ± 40 – 60 mV, in addition to weak but distinct hump features at biases ± 20 – 30 mV.

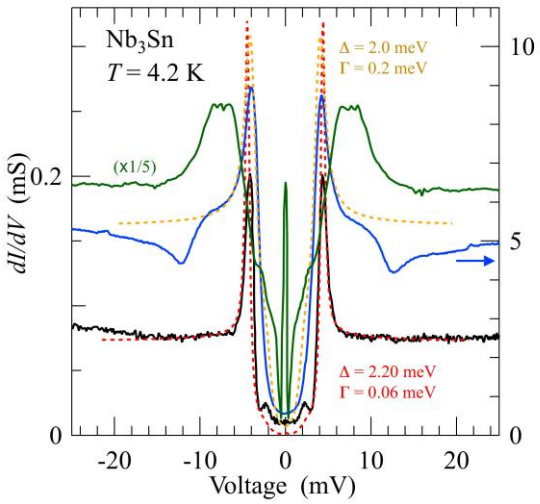

Fig.1. The tunnel conductance $G(V)$ of superconducting Nb_3Snjunctions obtained in break-junction tunnel-spectroscopy (BJTS)measurements. These spectra are obtained fordifferent junctionscorresponding to samples from the same batch. The dashed lines are the fitting results based on theBCSdensity of states $N(E,\Gamma)$ (see the details in the text).

In the top curve of Figure 2, the representative superconducting gap featureswithextra ± 20 mV humps areshown. The appearance of such features depends on the junction, i.e. they are often absent and not consistent with the superconducting gapat ± 4 – 6 mV. Therefore, itshould not berelated tosuperconductivity.This is alsoseen from Fig. 1, where there are no distinct features at around those bias voltages. The humps at ± 20 mVexhibit the weakchange, namely, 2 – 4 %, against the background. Such structures, whicharereproduced by our present measurements, werealready clearly observed and presented previously forNb-Sn break junctions [6]. Inthosedata, the peculiarities occurredbetween ± 20 mV and ± 30 mV. Such a subtle intensity could be associated with the strong electron-phonon interaction, which has been believed to be the most probablemechanism to inducesuperconductivity in Nb_3Sn and other A-15 compounds [15]. This is, however, not the case in the present measurements, because the peculiarities are too large to be the strong-coupling features. It should be emphasized that a caution against interpretation of the outer structures as strong-coupling effects was expressed earlier with the applicationto 5*f*-electron superconductor UPd_2Al_3[16].

An essential method to clarify the origin of such hump structures consists in finding of their temperature evolution. However, the BJTS are mechanically unstable. Hence, it is difficult to systematically measure temperature dependences of the structure concerned in the relevant regionpreserving the identical junction-interface properties.Nevertheless, we were able to follow the trace of the characteristic temperature evolution during the heating process. It is remarkable that the distinctpeak positions at about ± 20 mV, found at a low T = 4.2 K, i.e.much below T_c, remained the same during the heating. However, the peaks gradually transformed into heavily broadened and symmetric structuresclearly seenagainst the bias-dependent backgroundeven at temperatures 20.8 K. This temperature lies above the superconducting transition at 18 K. It means that these structures are not directly connected to superconductivity. The thermal smearing of the Fermi distribution function does not influence this broadened gap structure because the energy scale ~1.7 meV corresponding to the temperature 20.8 K is smaller as compared with that of the hump bias location at 20 meV (~ 240 K). The possible origin of gap-structures broadening is the effective widening of the junction area, so that the overall $G(V)$isformed by the averaging of the gap distributions. This conclusion is supportedby the observed relatively high conductance $G(V)$ magnitudes.

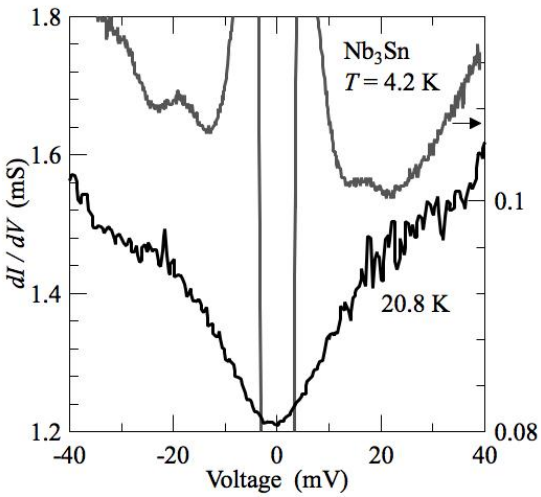

Fig.2. $G(V)$ of BJTS Nb_3Sn junctions in the superconducting state. These spectra are obtained from different junctions at 4.2 K and 20.8 K ($>T_c$).

We emphasize that the wider humps at ± 40 – 60 mV in the $G(V)$ curves are reproducible in addition to the above mentioned narrower features at V = ± 20 – 30 mV. Thesecharacteristics werediscovered in our previous BJTS measurements, in which merely the broadened humps or the shallow shouldersappearedin these bias voltage regions [8]. The repeated BJTS measurements at low temperatures confirmed the existence of the distinct gap-edge-like peaks among thecommonly observed weakhump or shoulder structures. Figure 3 demonstrates such an example, in which fairly discerniblepeaks appeared at ± 40 mV together with weaker but distinguishable peaks at ± 20 mV. We can therefore attribute the features at ± 40 mV as the dielectric gap

2Σ manifestations [8].The ± 40 mV peaksare in fact clearly visible, being10 percent higher thanthecorresponding background intensity. From these data, it is obvious that the distinct gap-like structures existwell above the superconducting gap energy, which supportsthe conclusion form the data of Figure 2. The finestructures at lower biases of |V| < 20 mV are probably associated with the superconductingweak-link formation with limited critical current density.

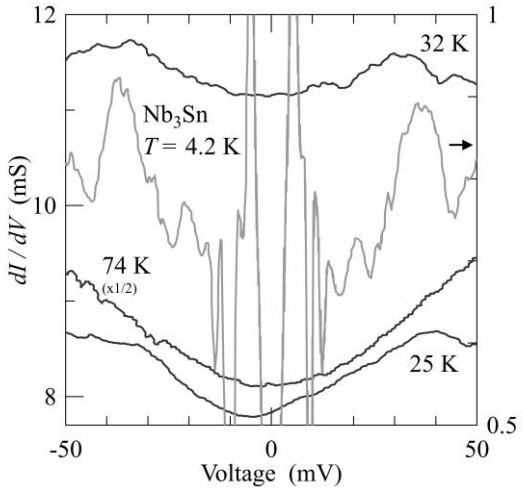

Fig.3. $G(V)$ of BJTS Nb_3Sn junctions in the superconducting and normal states. These spectra were obtained forvaryingjunctionproperties.

To obtain explicit temperature dependence of the high-bias feature constitutesaseparateproblem. We made attempts to clarify how the gap edge moves to lower biases. Unfortunately, the junction properties could not be stable throughout the temperature span.Nevertheless, we managed to observe the characteristics in almost the same patch of the broken junction. The results areshown in Figure 3.The spectral featuresscatter while temperature increases. One can see the gap-edge structures preservewell above $T_c$andgradually disappear, so that theycould not be observed above74K, where one sees only the substantially bias-dependent background. The fact that the high-energy gap-likefeatures do not disappear at $T_c$means that they are induced by such phenomena that exist both in the superconducting and normal state.Therefore, it seems improbable that ± 40 mV peculiarities are due to such precursor effects as fluctuating Cooper pairs. On the contrary, the interaction responsible for the gapping of the electron density of statesis presumably a phenomenon competing with the Cooper pairing for the Fermi surface.The substantial gap-related depression of $G(V)$ near zero bias above $T_c$indicates that the interface quality is sufficienttodetect thequasiparticle tunnel density-of-states evolution during various manipulations, including heating.

The temperature dependence of the gap values obtained from the data presented in Figure 3 is plotted in Figure 4. Since there are not enough data points, it is hard to draw definite conclusions about the thermal evolution of the gapfeatures.However, it is important that at least for this junction, the $G(V)$ curve exhibits no peculiar features at temperatures above 74 K.One should remind the fact that tunneling spectroscopy studies a realcontact interface, in which any subtle structures could be modified or suppressed due to the non-ideal electron scattering at the surface, especially when the temperature is increased inducingstrong thermal broadening of the Fermi distribution function. For this reason, it is very difficult to identify the exact gap closing temperature.

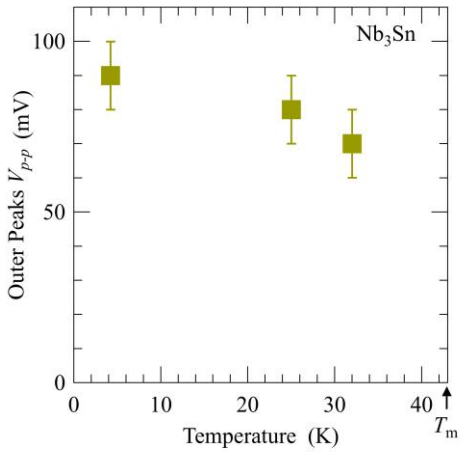

Fig.4. Temperature dependence of the outer peak-to-peak gap valuestaken from Fig. 3.

Nevertheless, one can recognize that the outer peak-to-peak distance $V_{p\text{-}p}$is reduced with the increase of temperature.Itshows the trend to close around the martensitic transition temperature T_m = 43 K of Nb_3Sn demonstrating a conventional mean-field gap evolution behavior. Since $V_{p\text{-}p}$= 4Σ/e, the conventional gap-to-$T_m$ratiocan be estimated as $2\Sigma/k_BT_m$~ 12, which is 3-4 times larger than the BCS mean field value.

The obtained value is typical for dielectric (CDW) transitions found in a number of materials [1,5].Moreover, the characteristicenergy scales and behavior of the normal-state gap observed here resemble the CDW gap formation and evolution in low dimensional conductors with the nesting sections on the Fermi surface [1,5,17]. Therefore, we believe that the superlatticeappears with the concomitant electron spectrum gapping driven by one of the mechanismssuggested for A-15 compounds [1-5]. Whatever the subtle theoretical details, therelevant phenomenon(the consequence of which is observed here)really occurs in A-15 compound Nb_3Sn and is known as the martensitic structural phase transition[2-4]. Below thecharacteristic temperatureT_m, the tetragonal periodic lattice distortions appeardeformingthe original cubic lattice.The transition isdriven by the Peierls-type instability due to displacement of Nb atoms. The concomitant CDW leads to the quasiparticle gap formation in the original electronic density of states $N(E)$. However, only a small Fermi surface section is affected and distorted by the dielectric energy gap created by this transition. Since the electron spectrum changesarerelatively weak, the electronic transport

properties arenot significantly affected as is confirmed bythe experiment[8]. Therefore, not so muchattention was paid previouslyto the peculiarities of the tunnel conductance spectra characterizing Nb_3Sn tunnel junctions. Moreover, CDW distortions in Nb_3Sn seem to be spatially inhomogeneous similarly to what is inherent to cuprate layered structures [1, 10]. This would make the electron spectrum due to the CDW instability much smoother than in conventional types of sharp second-kind phase transitions. Therefore, the CDW gapping reveals itself in the tunnelingconductance $G(V)$ as a weak pseudogap-like feature well known for other objects [1, 10]. This is readily understood taking into account the inhomogeneity effects and the gapping of only a small Fermi surface section[1].

In order to investigate the gap structure of Nb_3Snmore thoroughly and systematically, the comparable measurementsof STM/STS were carried out.In fact, as far as we know, there was merely a preliminary report on STM/STS measurements presented 3 decades ago [19]. The technical difficulty in the measurements of A-15 cubic compounds like Nb_3Sn is the lack of apparent cleave plane in the crystal. This is a fatal weakness of the scanning measurements using this kind of the samples. One should remind that there are enormous numbers of reports on the STM/STS measurements of the conventional and novel superconductors, but unfortunately all of them were done using layered compounds and/or thin films in which the surface states differ substantially from their bulk counterparts. In what follows, we describe the STM/STS measurements of Nb_3Sn.

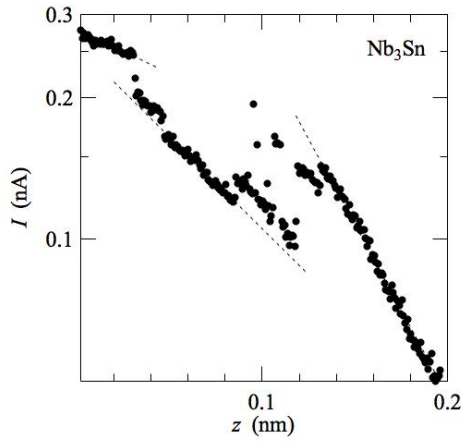

Fig. 5. Dependence of vacuum tunneling current I on the PtIr tip – Nb_3Sn sample distance at T = 4.9 K.

Figure 5 demonstrates the dependence of tunneling current I on the tip-sample distance z, as the initial procedure of the STM measurements. The Nb_3Sn sample is taken from the same batch as was used for the BJTS measurements. The data points are strongly scattered. The work functionϕ, the magnitude of which characterizes the quality ofthe crystal surface flatnesscan be recovered, in principle, fromour $I(z)$ dependences measured by STM/STS. Since the present sample does not possess the layered structure, one should not expect the requiredatomic flatness of the crystal surface. This must be the major reason of the data scatter in Fig. 5. Nevertheless, the conventional exponential $I(z)$ dependences are obtained insome surface areas. From corresponding $I(z)$,rough estimations of ϕ are possible. The estimated values of ϕ thus obtained are in the range 0.7–3.2eVfor z < 0.2 nm. As comes about from the data, for smaller z the work function ϕ is lower, the changes occurring abruptly. Thereason may be non-trivial.Namely, the work function reflects the degree of surface roughness.On the other hand, the shorter is the electron tail outside the conducting sample,the higher should be the corresponding ϕ value.In the vicinity of the rough interface (small z) the electron density in the vacuum in some patches may be larger than for the smooth interface. Hence, the apparent ϕ is reduced. On the contrary, for largerzthe influence of atomic corrugationsis smoothed out, so that the natural electronic conditions with the intrinsic, larger, ϕ are restored.As a result, the measured work functionϕ andits z-dependenceare fairly good characteristicsof the surface properties.At the same time, in the purely layered superconducting material nearly ideal values of ϕ =3 –5 eVwere found [20].

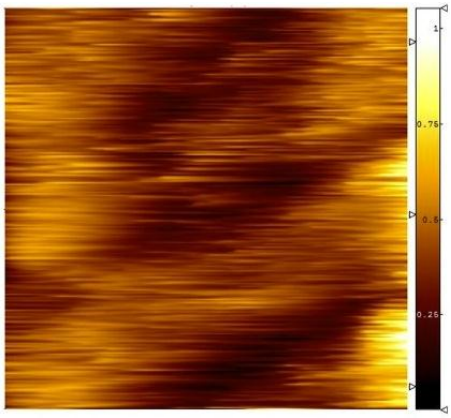

Fig. 6. STM image of the *in situ* cracked surface of Nb_3Sn at T = 4.9 K.The scanning area is 10 nm × 10 nm,V = 0.1 V and I= 0.4nA. Vertical bar on the right side indicates the relative height of the topography (the brighter is the higher).

Figure 6 demonstratesa trial STM topographymeasured on the Nb_3Sn surface.To our knowledge, this is the first STM observationof the A-15-compound surface obtained here for a small area of 10 nm × 10 nm.This circumstance justifies thecurrent presentation notwithstandingitstopography non-atomic resolution. As is expected from the I-z characteristics shown in Figure 5, it was difficult to resolve the surface atomic arrangements. Nevertheless, the image shown here was reproducedduring other scanning runs. In this STM image, there are contrastingstripes running inthe diagonal direction. The period of the stripes is about 3.5 nm, which corresponds to 6.5 times unit cell constanta_0.At present, the detailed features of the stripes, which may have either electronic or atomic origin, are not known, but the stripe existence seems to argue in favor of the normal-state gapping found in this compound. It is alsointeresting to note that the period of those stripes is similar to that observed on the surface of high T_c superconductors [1].

Figure 7 shows $G(V)$ measured for Nb_3Sn in the STSmode.Thesuperconducting-gap like structure is clearly visible at 4.9 K. In principle, the gap-edge peaks in the SIN junction (similar to thosein the STS one) occur athalf the peak interval of BJTS. However, in the presented data, the $V_{p\text{-}p} \approx 16$ mVis larger than what was expected from the BJTS, although the samples originated from the samebatch. Since the peak positions identified with the gap-edgelocations are often overestimated in the broadened spectra, we adopted the fitting procedure using the $N(E,\Gamma)$ in the SIN configuration. The result indicates the gap value of $2\Delta \approx 10$ meV, which is smaller than the observed $eV_{p\text{-}p}$, but it is still much larger than that from the $2\Delta \sim 3$ meV of the BJTS. Another discrepancy between the experimental and calculated curves is the hugeleakage in the sub-gap region around zero bias, which could not be reproduced even by increasing the broadening parameter Γ.Such a situation may be a result of simultaneous probing ofthe non-gapped nanometer-size domains.

When the bias voltage is increased, another characteristic feature appeared, which is the broad hump structures at the biases of ± 40 – 50 mV. These features must correspond to the normal state gap observed in the BJTS, but the hump positions of ± 40 – 50 mV in STS hereare the same as $\pm 2\Sigma/e$ of the BJTS, in spite of the expected $\pm 4\Sigma/e$. Thishigh-bias hump feature was already observed in the Nb_3Sn – metal junction without noticing as the gap-edge structure [15].The presented STS measurementsraiseissues to be clarified in the future.

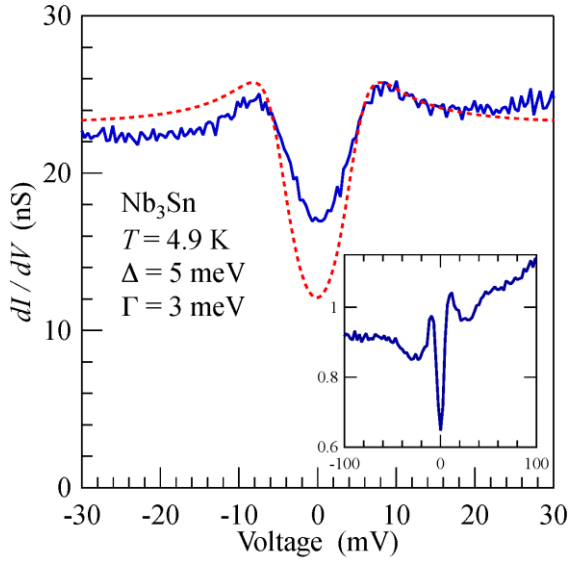

Fig. 7.Tunneling conductance $G(V)$ in the superconductinggap region measured by STS. The inset shows the high-bias feature.

The coexisting superconducting-gap and hump structures presented here in Nb_3Sn are very similar to those found in the tunneling-conductance characteristics of high-$T_c$cuprates and recently reported iron-chalcogenides except for the energy scales[1, 14, 21]. These apparent similaritystimulates further studies to compare the objects concerned, whichwe are going to study in more detail.

III. Conclusion

The classical superconductor Nb_3Sn wasstudied by break junctionand scanning microscopy/spectroscopytunneling techniques. We observed superconducting-gap structuresofthe BCS size and the humps most probably being a manifestation of the normal state gap, accompanying the martensitic phase transition. The low-temperature humps outside the superconducting gap obtained by break-junction tunneling are confirmed by thepreliminary STM/STS measurements. There is the apparent discrepancy in the energy scales between BJTS and STM/STS, whichwaits forclarification.The resultant normal gap to transition temperature ratio from the BJTS is similar to that found inthe low-dimensional conductor $NbSe_3$, which was studied decades ago. These results strongly suggest that the normal-state gap is induced by the Peierls-type instability ubiquitousto low-dimensional electron structures, in which nested sections of the Fermi surfaceare removed below the structural transition. Similar CDW-like phenomena were observedincupratesboth directly and asthe pseudogapmanifestations. They were also found in the novel iron-chalcogenide superconductors together with spin-density waves [22].In all such materials CDW gaps close at temperatures higher than the superconducting critical one, although both order parameters coexist at temperatures lower than T_c.

References

[1] A.M. Gabovich, A.I. Voitenko, T. Ekino, M.S. Li, H.Szymczak, M. Pekala, Adv. Condens. Matter Phys. **2010**, 681070, 2010.
[2] L.R. Testardi, Rev. Mod. Phys. **47**, 637, 1975.
[3] L.P. Gorkov, Zh. Eksp. Teor. Fiz. **17**, 525, 1973.
[4] G. Bilbro, W.L. McMillan, Phys. Rev. B**14**, 1887, 1976.
[5] A.M. Gabovich, A.I. Voitenko, M. Ausloos, Phys. Rep. **367**, 583, 2002.
[6] J. Moreland, J.W. Ekin, J. Appl. Phys. **58**, 3888, 1985.
[7] R. Escudero, F. Morales, Solid State Commun.**150**,715, 2010.
[8] T. Ekino, A. Sugimoto, Y. Sakai, A.M. Gabovich, J.Akimitsu, Low Temp. Phys. **40**, 1182, 2014.
[9] T. Ekino, T. Takabatake, H. Tanaka, H. Fujii, Phys. Rev. Lett. **75**, 4262, 1995.
[10] T. Ekino, A. M. Gabovich, M. S. Li, M. Pękała, H. Szymczak, A. I. Voitenko, Phys. Rev. B **76**, 180503, 2007.
[11] M. Marz, G. Goll, W. Goldacker, R. Lortz, Phys. Rev. B **82**, 024507, 2010.
[12] R.C. Dynes, V. Narayanamurti, J.P. Garno, Phys. Rev. Lett.**41**,1509, 1978.
[13] T. Ekino, H. Fujii, M. Kosugi, Y. Zenitani, J. Akimitsu,Phys. Rev. B **53**, 5640, 1996.
[14] T. Ekino, K. Nagasaka, Y. Sakai, A. Sugimoto, A.M. Gabovich, Phys.Procedia**65**, 65, 2015.
[15] J. Geerk, U. Kaufmann, W. Bangert, H. Rietschel, Phys. Rev. B **33**, 1621, 1986.
[16] J. Geerk, H.v. Lohneysen, Phys. Rev. Lett. **99**,257005, 2007.
[17] T. Ekino, J. Akimitsu, Jpn. J. Appl. Phys. Suppl. **26**, 625, 1987.

[18] P. Monceau, Adv. Phys. **61**, 325, 2012.
[19] A.L. de Lozanne, S.A. Elrod, C.F. Quate, Phys. Rev. Lett.**54**, 2433, 1985.
[20] A. Sugimoto, K. Shohara, T. Ekino, Z. Zheng, S. Yamanaka, Phys. Rev. B **85**, 144517, 2012.
[21] T. Ekino, Y. Sezaki, H. Fujii, Phys. Rev. B **60**, 6916, 1999.
[22] A. Sugimoto, T. Ekino, A. M. Gabovich, Phys. Rev. B **90**, 224503, 2014.